J. Fluid Mech. (2004), *vol.* 517, *pp.* 199–208.
DOI: 10.1017/S0022112004000904 Printed in the United Kingdom

Maximal deformation of an impacting drop

By CHRISTOPHE CLANET[1], CÉDRIC BÉGUIN[1], DENIS RICHARD[2] AND DAVID QUÉRÉ[2]

[1]Institut de Recherche sur les Phénomènes Hors Equilibre, UMR 6594, 49 rue F. Joliot Curie, B.P. 146, 13384 Marseille, France

[2]Laboratoire de Physique de la Matière Condensée, URA 792 du CNRS, Collège de France, 75231 Paris Cedex 05, France

(Received 12 March 2004 and in revised form 10 June 2004)

We first study the impact of a liquid drop of low viscosity on a super-hydrophobic surface. Denoting the drop size and speed as D_0 and U_0, we find that the maximal spreading D_{max} scales as $D_0 We^{1/4}$ where We is the Weber number associated with the shock ($We \equiv \rho U_0^2 D_0/\sigma$, where ρ and σ are the liquid density and surface tension). This law is also observed to hold on partially wettable surfaces, provided that liquids of low viscosity (such as water) are used. The law is interpreted as resulting from the effective acceleration experienced by the drop during its impact. Viscous drops are also analysed, allowing us to propose a criterion for predicting if the spreading is limited by capillarity, or by viscosity.

1. Introduction: bouncing drops

Texturing a hydrophobic material (such as a wax) makes it super-hydrophobic, i.e. provides a contact angle for water as high as 160° to 170° (Onda *et al.* 1996). This effect is primarily due to the presence of air remaining on the solid as a drop is deposited, which increases dramatically the contact angle and decreases the adhesion of the liquid to its substrate. This has an amusing consequence, of practical importance: the impact of a water drop on such a substrate can be followed by a rebound (Hartley & Brunskill 1958). The restitution coefficient of the shock can be very large (around 0.9), so that a drop can bounce many times before stopping (Richard & Quéré 2000). On a super-hydrophobic plant such as the lotus, where the leaves are tilted, this provides a very efficient way to remove the rain, as the drops are scattered onto the ground.

Our first aim here is to describe more precisely the shock, using a high-speed video camera. We examine how the drop deforms during impact, as a function of the drop velocity, size and viscosity. A rebound is possible because the kinetic energy of the impinging (non-viscous) drop can be stored in deformation during the impact. Thus, a natural parameter to be considered is the so-called Weber number We, which compares kinetic and surface energy. For a drop of diameter D_0, a liquid of surface tension σ and density ρ, and an impact velocity U_0, the Weber number is

$$We = \frac{\rho U_0^2 D_0}{\sigma}. \tag{1.1}$$

For Weber numbers smaller than unity, the deformation is small: the drop is ellipsoidal during the contact (Richard & Quéré 2000; Okumura *et al.* 2003). For We larger than 1, the situation is quite different, as can be observed in figure 1.

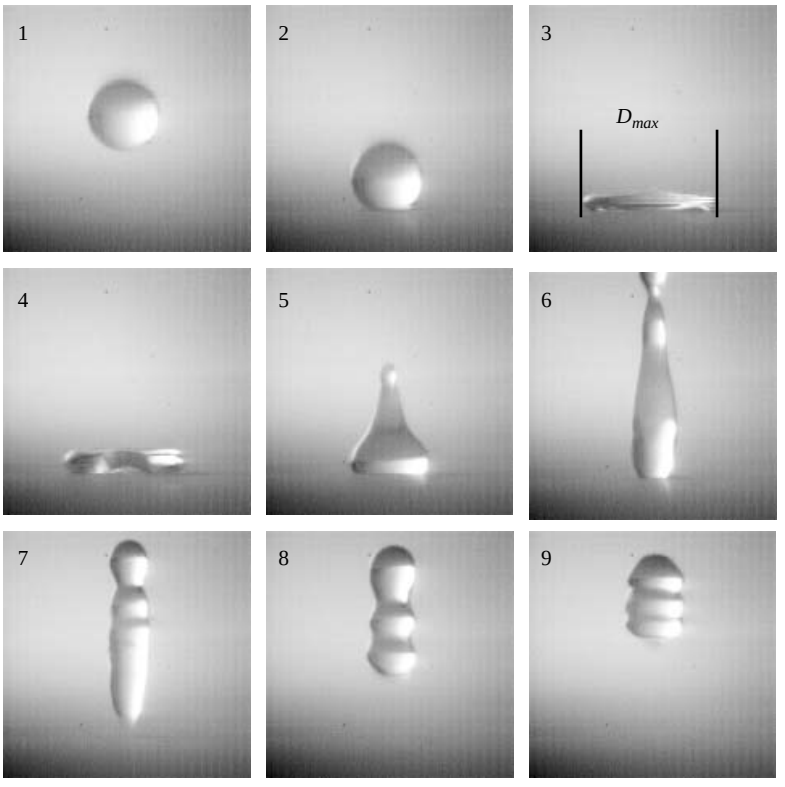

FIGURE 1. Impact of a water drop ($D_0 = 2.5\,\text{mm}$, $U_0 = 0.83\,\text{m s}^{-1}$) on a super-hydrophobic surface. Time interval between the pictures: 2.7 ms.

The snapshots display the impact of a water drop ($D_0 = 2.5\,\text{mm}$) on a solid (on which the static contact angle is 170°) at a speed $U_0 = 0.83\,\text{m s}^{-1}$, which yields $We = 24$. The second picture of the series shows the (spherical) drop just at impact, which defines $t = 0$. Picture 3 is taken at $t = 2.7\,\text{ms}$, and indicates that the drop is flattened as it reaches its maximal extension $D_{max} \approx 2D_0$. Then, it retracts and takes off (picture 7), at $t = \tau = 13.5\,\text{ms}$. The drop is not spherical at that moment, so that it oscillates once in the air (which is mainly responsible for a restitution coefficient smaller than unity) (Richard & Quéré 2000). Note also that the contact angle during the contact ($t < \tau$) remains close to its maximal value π.

The contact time has been studied (Richard, Clanet & Quéré 2002; Okumura *et al.* 2003) and shown to scale as $\sqrt{\rho D_0^3/\sigma}$. This variation, independent of the impact velocity U_0, can be understood by considering (globally) the rebound as an oscillation: the drop is a spring of stiffness σ and mass ρD_0^3, which oscillates with a constant period $\sqrt{\rho D_0^3/\sigma}$.

Our aim here is to describe the size of the puddle formed at the maximal extension, D_{max}. We first measure the maximal deformation of the impinging drop, and examine our results using scaling arguments. More generally, we discuss the characteristics of a drop experiencing an acceleration γ. Then, we show whether our results are modified when considering impacts on more common surfaces, and with more viscous liquids.

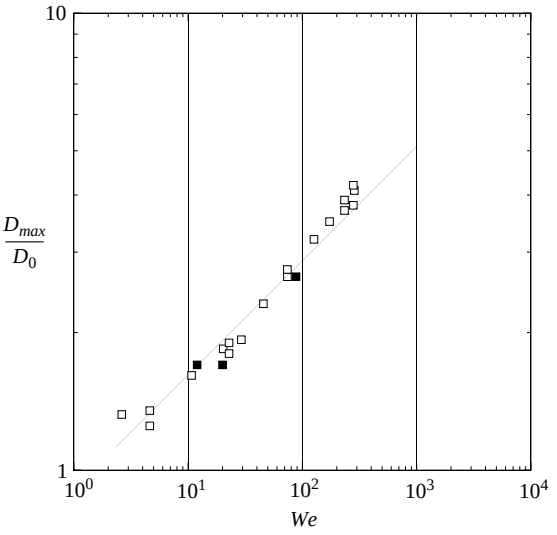

FIGURE 2. Maximum diameter of the spreading drop (deduced from photos such as displayed in figure 1), normalized by the drop radius, as a function of the Weber number. The open squares are obtained with water, and the filled ones with mercury. The solid line indicates the slope 1/4.

2. Maximal deformation on a super-hydrophobic surface

2.1. *Impacting drops*

The maximum diameter D_{max} was measured for water and mercury drops hitting a super-hydrophobic substrate. This quantity was observed to increase with both the drop radius and the impact speed. All the data were found to collapse on a single curve, when plotting D_{max}/D_0 as a function of the Weber number, as shown in figure 2. In logarithmic scales, the data are well fitted by a straight line of slope 0.27 ± 0.02, suggesting that D_{max} scales as $We^{1/4}$, and thus as $U_0^{1/2}$.

This behaviour is very different from that reported up to now. The most classical proposition is that the kinetic energy of the impinging drop (of the order of $\rho D_0^3 U_0^2$) is dissipated by viscosity during the impact (the associated energy dissipation scales as $\eta(U_0/h)D_{max}^3$, h being the thickness of the maximal drop). Together with volume conservation ($hD_{max}^2 \sim D_0^3$), this yields $D_{max} \sim D_0 Re^{1/5}$, introducing the Reynolds number $Re \equiv \rho D_0 U_0/\eta$ (Chandra & Avedisian 1991; Rein 1993). The maximum diameter thus increases as $U_0^{1/5}$, a much smaller dependence than the one reported here. Hence our results raise the question of the validity of this kind of model in the limit of liquids of low viscosity considered here.

On the other hand, in such a limit, and with super-hydrophobic substrates which also contribute to minimize viscous dissipation (because of a very high contact angle), we could expect a pure transfer of kinetic energy into surface energy (Richard *et al.* 2002), an idea strengthened by the existence of rebounds. In the limit of large Weber numbers (for which we can neglect the surface area of the drop edge), this energy conservation is simply $\rho D_0^3 U_0^2 \sim \sigma D_{max}^2$. This yields $D_{max} \sim D_0 We^{1/2}$ ($D_{max} \sim U_0$), which clearly is not the law obeyed by the data (in particular at large We, as assumed above).

In a stage of maximal deformation, the drop is flattened, and looks like a small-scale model of a gravity puddle, made by pouring a large water drop onto a wax surface. More precisely, this shape is observed if gravity overcomes surface tension,

i.e. if the drop is larger than the capillary length $a \equiv \sqrt{\sigma/(\rho g)}$ (in practice a is 2.7 mm for water and 1.9 mm for mercury). Since the shape of the puddle results from a balance between gravity and surface forces, its thickness necessarily scales as a, the prefactor being a monotonic function of the contact angle (Taylor & Michael 1973). The idea here is that the velocity of a drop hitting a solid decreases from U_0 to 0, in a crashing time $\tau^\star$ of the order of D_0/U_0. Thus the typical acceleration γ experienced by the drop as it stops scales as U_0^2/D_0, which in our experiments ($U_0 \sim 1\,\mathrm{m\,s^{-1}}$ and $D_0 \sim 1\,\mathrm{mm}$) is commonly about 100 times larger than g. The thickness of a puddle in this reinforced gravity field should scale as $a^\star = \sqrt{\sigma/(\rho\gamma)}$. With $\gamma \sim U_0^2/D_0$, and using volume conservation, we deduce a maximum diameter:

$$D_{max} \sim D_0 We^{1/4} \tag{2.1}$$

in good agreement with the data in figure 2, where (2.1) is as a solid line (with a numerical coefficient equal to 0.9).

This dynamic argument allows us to understand the special shape of a drop as it stops after an impact (it forms a puddle because of an effective gravity field U_0^2/D_0), and the resulting scaling law for the maximal spreading. It also implies that a drop smaller than $a^\star$ should not form a puddle: then, surface forces dominate 'gravity' forces, so that the drop should be closer to a sphere. The condition $D_0 < a^\star$ implies $We < 1$, and we stress that a drop in this regime indeed forms an ellipsoid during the shock (Richard & Quéré 2000). Note also that (2.1) can only hold if the crashing time $\tau^\star \sim D_0/U_0$ is smaller than the contact time τ of the drop, which was shown to scale as $\sqrt{\rho D_0^3/\sigma}$. This imposes (again) the condition that the Weber number be larger than unity. In addition, for $2 < We < 900$ we checked that the maximal spreading is indeed reached in a time which scales as D_0/U_0 (with a numerical coefficient of 0.6 ± 0.1).

Let us finally emphasize that the scaling in (2.1) is compatible with Euler's equation. Written dimensionally, this equation expresses the balance of an acceleration (of the order of $\rho U_0/\tau^\star$, that is, $\rho U_0^2/D_0$) with a pressure gradient, which is in that case the Laplace pressure gradient tending to restore a spherical drop (and thus scaling as σ/h^2, with h the puddle thickness) (Okumura *et al.* 2003). Together with volume conservation, this balance yields (2.1).

2.2. *Drops on a lift*

Our interpretation can be tested by considering (more generally) the shape of a drop experiencing an imposed acceleration γ. This can be achieved using a lift: a spherical drop is deposited on a super-hydrophobic plate (where it is quasi-spherical), and the whole device is suddenly accelerated upwards. Our lift consists of a spring initially compressed, as sketched in figure 3. At $t = 0$, the hook G is removed, and the drop is moved upward. An example of lift trajectory is presented in figure 3(*c*). Using a parabolic fit, we observe that the acceleration is quasi-constant and equal to $120\,\mathrm{m\,s^{-2}}$ over the first 18 ms. The deformation obtained with this spring for a drop of diameter $D_0 = 3.1\,\mathrm{mm}$ is displayed in figure 4. As for the impact, the drop flattens, reaches a maximal extent $D_{max} \approx 1.7 D_0$ (picture 6) prior to retraction. In this example, the drop reaches its maximal extension at $t \approx 7\,\mathrm{ms}$, that is within the range of constant acceleration. This was the case for all the experiments reported.

The relative deformation D_{max}/D_0 of water drops of various diameters and for accelerations between $\gamma = 93$ and $580\,\mathrm{m\,s^{-2}}$ is plotted in figure 5, as a function of the dimensionless acceleration $\rho\gamma D_0^2/\sigma$. The data follow a scaling law similar to the one in figure 2, which yields $D_{max} \sim D_0\,(\rho\gamma D_0^2/\sigma)^{1/4}$. A close comparison with the data in

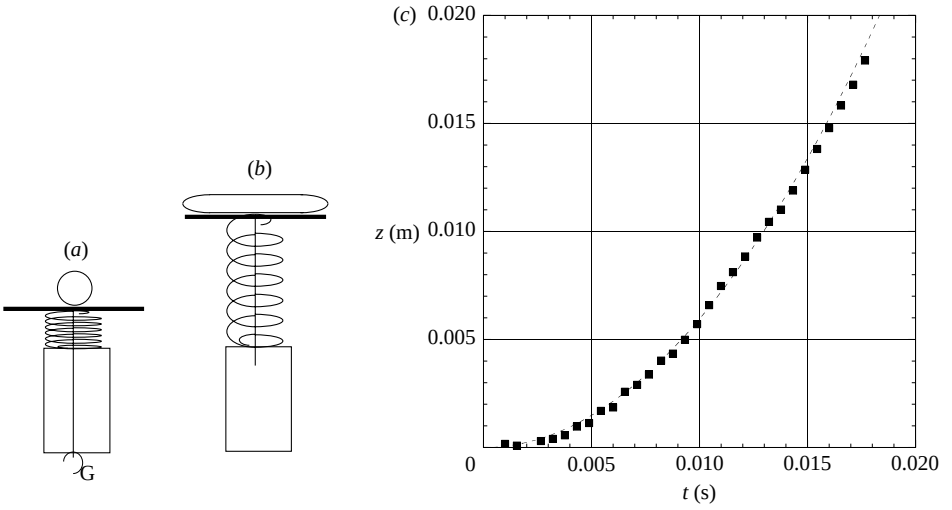

FIGURE 3. (*a*) Sketch of the lift used to study the deformation of a drop experiencing a constant acceleration γ larger than the gravitational acceleration. The upper plate is a super-hydrophobic material. (*b*) At time $t = 0$, the hook G is removed, and the spring suddenly loses its tension. The whole experiment is filmed with a high-speed camera, allowing us to measure γ and the drop deformation. (*c*) Example of lift trajectory (■) corresponding to the experiment reported in figure 4. The dashed line corresponds to the fit $z = 60t^2$, that is to an acceleration of $120\,\mathrm{m\,s^{-2}}$.

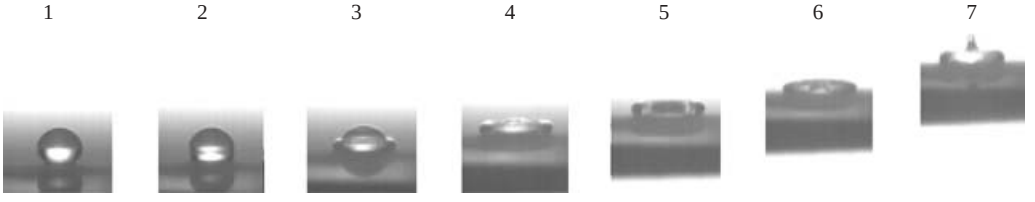

FIGURE 4. Deformation of a water drop (of diameter $D_0 = 3.1\,\mathrm{mm}$) sitting on a super-hydrophobic plate, and subjected to a constant acceleration $\gamma = 120\,\mathrm{m\,s^{-2}}$. The time interval between the pictures is 1.6 ms.

figure 2, shows that the drop indeed undergoes the same relative deformation in both experiments provided that the acceleration of the lift is chosen such that $\gamma \sim U_0^2/D_0$.

2.3. *Energy conservation*

The maximal deformation of an impacting drop in the capillary regime was found to scale as $We^{1/4}$, which implies (for $We > 1$) an extension smaller than given by energy conservation (then, D_{max} increases as $We^{1/2}$). Thus kinetic energy is not purely transformed to surface energy during the shock, which raises the question where the missing energy is stored (which is all the larger since We is high). To answer this question, we tried to visualize the flow inside the drop during the impact. Observations were very difficult to interpret with such small systems as millimetric drops, and we considered balloons filled with water, in order to enlarge the system. Provided that the experimental conditions were carefully chosen, the shock of the balloon ($D_0 = 31.5\,\mathrm{mm}$,

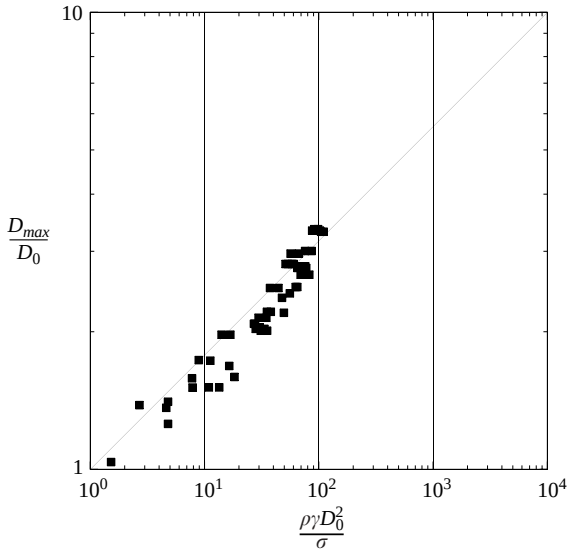

FIGURE 5. Relative deformation D_{max}/D_0 of a water drop in a lift, as a function of the dimensionless lift acceleration $\rho\gamma D_0^2/\sigma$. The scales are the same as in figure 2, and the solid line indicates the slope 1/4.

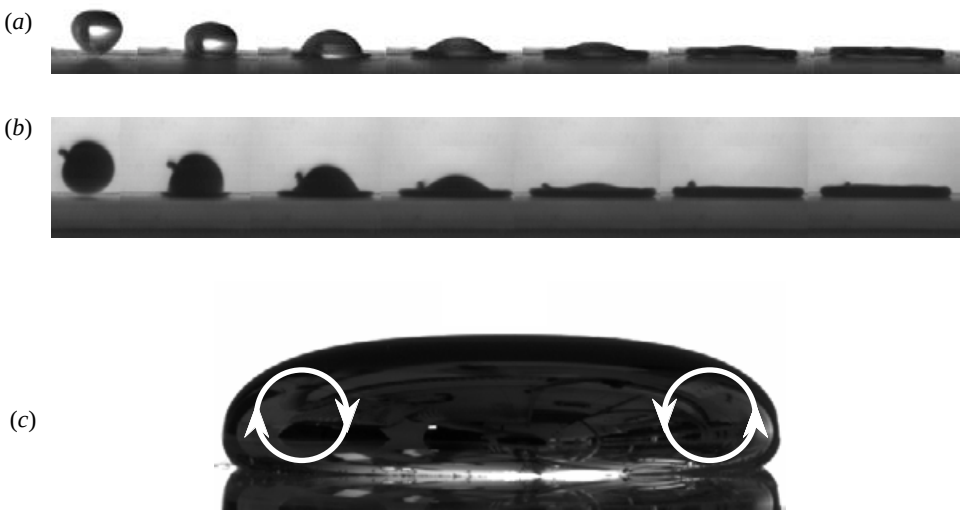

FIGURE 6. (*a*) Impact of a water drop ($D_0 = 2.9\,\text{mm}$, $U_0 = 1\,\text{m s}^{-1}$, $\sigma = 0.07\,\text{kg s}^{-2}$). (*b*) Impact of a balloon filled with water ($D_0 = 31.5\,\text{mm}$, $U_0 = 14.47\,\text{m s}^{-1}$, $\sigma = 85\,\text{kg s}^{-2}$). For these parameters, the shock is observed to be the same. (*c*) Sketch of the vortical motion revealed by the presence of tracers inside the balloon.

$U_0 = 14.5\,\text{m s}^{-1}$ and $\sigma \approx 85\,\text{kg s}^{-2}$†) was found to be very close to the one observed with a water drop ($D_0 = 2.9\,\text{mm}$, $U_0 = 1\,\text{m s}^{-1}$ and $\sigma \approx 0.072\,\text{kg s}^{-2}$), as shown in figures 6(*a*) and 6(*b*).

† As shown in Richard & Quéré (2000), an equivalent surface tension for a balloon can be deduced from the static deformation of the balloon under a known compression.

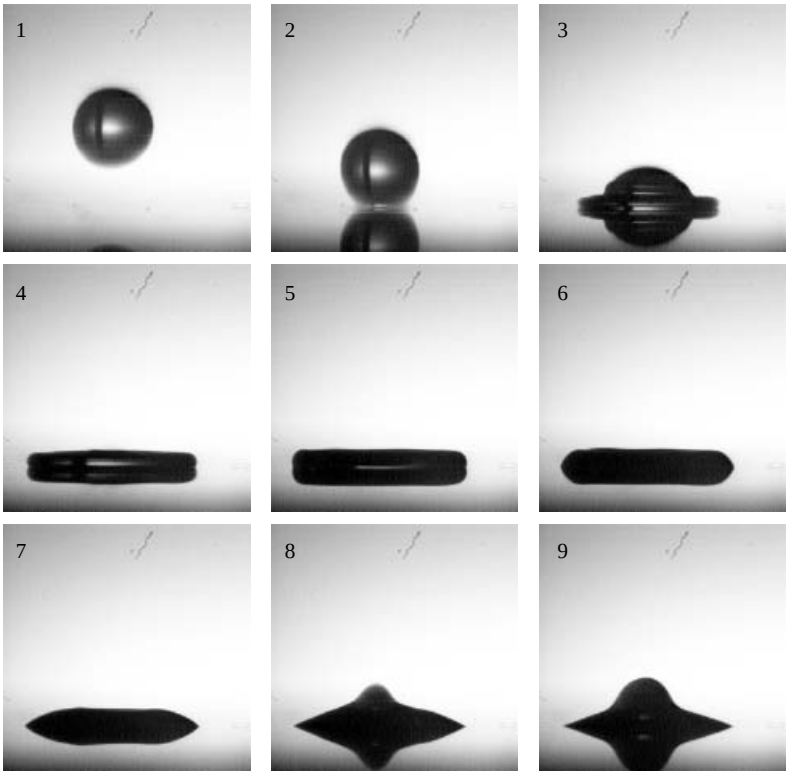

FIGURE 7. Impact of a water drop ($D_0 = 3.3\,\text{mm}$, $U_0 = 0.81\,\text{m s}^{-1}$) on a plastic that it wets only partially (advancing and receding angles of $92 \pm 2^\circ$ and $23 \pm 2^\circ$). The drop retracts but does not bounce. Time interval between the pictures 2.2 ms.

A rubber balloon can be transparent, and use of tracers reveals internal motion during the shock. These motions were found to be vortical, as sketched in figure 6(*c*), and observed as the balloon reaches its maximal extension. Thus, the kinetic energy is not only transformed to surface energy, but also to internal kinetic energy, which might help in understanding why a simple energy conservation does not hold.

3. Remarks

3.1. *Influence of the surface*

A drop hitting a surface first spreads inertially, whatever the nature of the surface. For liquids of low viscosity (such as water), it is thus tempting to test (2.1) on substrates which are not super-hydrophobic. An example of a water drop impact on plastic is displayed in figure 7. Then, the wetting is only partial with an advancing angle of $92 \pm 2^\circ$, and a receding one of $23 \pm 2^\circ$. The drop diameter is $D_0 = 3.3\,\text{mm}$ and the impact speed $U_0 = 0.81\,\text{m s}^{-1}$.

The drop reaches maximal extension $D_{max} \approx 2.1 D_0$ in picture 5. It does not bounce, and its shape in the receding stage (pictures 6 to 9) is clearly different from those in the super-hydrophobic case (figure 1). Nevertheless, the maximal extension is also found to obey (2.1), as shown in figure 8(*a*) where our data on plastic (filled squares) are superimposed on the data obtained on a super-hydrophobic plate (open squares). This can be confirmed by including in figure 8(*a*) the maximal extension of a water

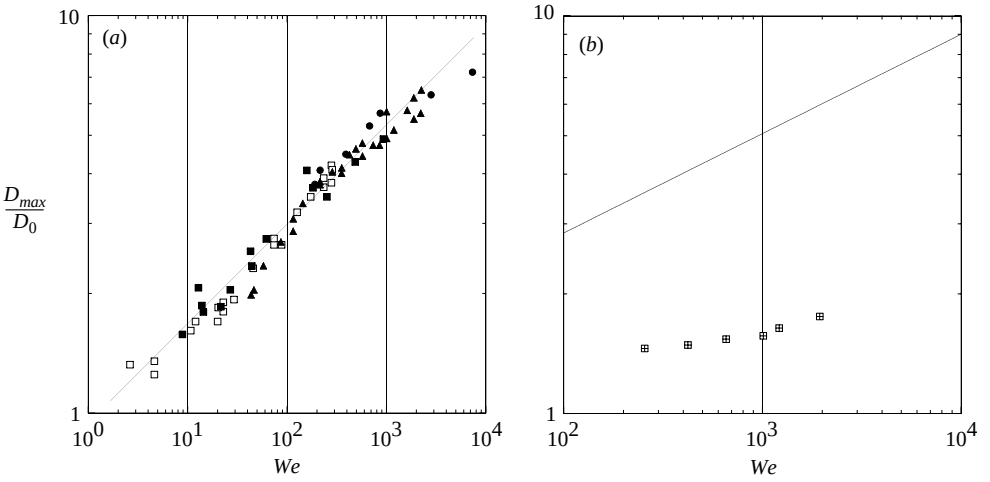

FIGURE 8. (*a*) Comparison between the relative deformation of a water drop impacting a super-hydrophobic surface (□) and a partially wettable surface (■). Also shown are data obtained by Stow & Hadfield (1981) for water impacting a smooth aluminium plate (●), and by Marmanis & Thoroddsen (1996) for water impacting thick linen paper (▲). All the data are found to be superimposed, and to be described by (2.1). (*b*) Comparison between the results obtained with water (or mercury), and described by (2.1) (solid line), and data obtained with a drop of silicone oil of viscosity $\eta = 300$ mPa s impacting a smooth plastic surface. The deformation of the drop is found to be (as expected) greatly reduced by the effect of viscosity.

drop impinging on a smooth aluminium plate (data by Stow & Hadfield 1981), filled circles), or thick linen paper (data by Marmanis & Thoroddsen 1996, filled triangles).

3.2. *Transition to a viscous regime*

All these results only hold if the impinging liquid has a low viscosity. Conversely, we expect the spreading of a viscous drop to be limited by the effect of viscosity, which yields (as shown in § 2.1) $D_{max} \sim D_0 Re^{1/5}$. More generally, the maximum diameter should be the small of that and the one given by (2.1). We can thus define an impact number $P \equiv We/Re^{4/5}$, and the inviscid case considered up to now implies a small P ($P < 1$). This condition was indeed satisfied in the experiments (for which $P < 0.3$). Using a viscous liquid with similar impact speeds and drop sizes should modify dramatically the observed behaviour, which is shown in figure 8(*b*). There, we compare to (2.1) the results obtained with a silicone oil of viscosity $\eta = 300$ m Pa s impinging on a smooth plastic surface ($P > 50$). The maximal deformation is found to be much smaller (by a factor between 2 and 5) than predicted by (2.1) (drawn as a solid line), with a much slower dependence on the velocity.

The viscous regime can be characterized by plotting the maximal deformation as a function of the Reynolds number, as done in figure 9, using our data (silicone oils of viscosity $\eta = 20$ and 300 mPa s) and Thoroddsen's for three mixtures of water and glycerol (Marmanis & Thoroddsen 1996). The law $D_{max} \sim D_0 Re^{1/5}$ is drawn as a solid line, and found to fit quite well the whole set of data. The transition between the capillary and the viscous regime is shown in figure 10, where the dimensionless viscous extension $D_{max}/(D_0 Re^{1/5})$ is plotted as a function of the impact number $P = We/Re^{4/5}$, for all our measurements. The transition between the two regimes is very clean. It occurs around $P = 1$, as expected, since all the numerical

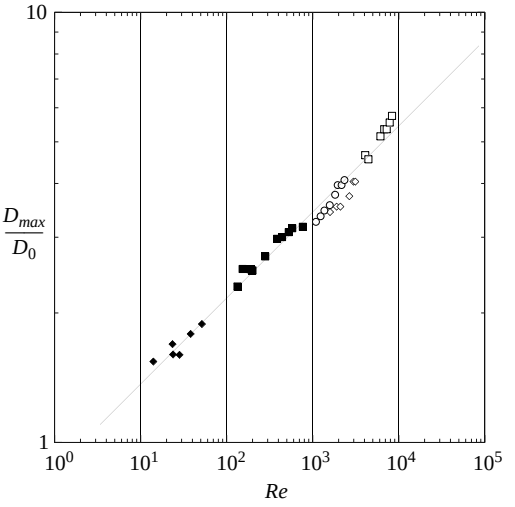

FIGURE 9. Relative deformation of viscous drops, as a function of the Reynolds number Re ($Re \equiv \rho D_0 U_0/\eta$), for silicone oils (◆, $\eta = 300$ mPa s; ■, $\eta = 20$ mPa s), and results by Marmanis & Thoroddsen (1996) for three viscous solutions of water and glycerol (open symbols). The points are fitted well by the law $D_{max} \sim D_0 Re^{1/5}$, drawn as a solid line.

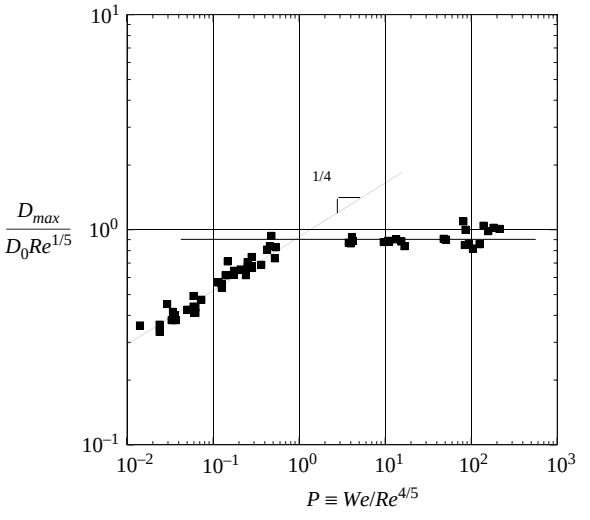

FIGURE 10. Dimensionless deformation of an impinging drop (where the maximal extension D_{max} is normalized by the maximal deformation in the viscous regime $D_0 Re^{1/5}$), as a function of the impact number $P = We/Re^{4/5}$, for all our measurements. Two regimes are followed, which successively correspond to the capillary regime (Eq. 2.1) and to the viscous one ($D_{max} \sim D_0 Re^{1/5}$). The transition occurs around $P = 1$.

coefficients were (experimentally) observed to be very close to unity. Since P scales as $\rho^{1/5} D_0^{1/5} U_0^{6/5} \eta^{4/5} \sigma^{-1}$, the capillary regime ($P < 1$) is likely to be observed at small velocities, for small viscosities and large surface tension. On the other hand, the capillary regime is found to be nearly independent of the drop size (since P varies as $D_0^{1/5}$).

4. Conclusion

We address in this paper the question of the maximal extension of an impinging drop, a question of practical importance since it defines the mark made on a solid by such drops. In the limit of low viscosity and low wettability (water on a superhydrophobic surface), we found that the maximum diameter of the drop in its spreading stage scales as $D_0 We^{1/4}$, where We is the Weber number associated with the impact. This law was found to hold on more wettable surfaces, and interpreted as resulting from the equation of motion: during the shock the drop experiences an effective acceleration much more intense than the gravity field, which flattens it and fixes its extent.

The case of more viscous liquids was also analysed, and a criterion for predicting if the spreading is limited by capillarity or by viscosity was derived. Questions remain, the most interesting, in our opinion, being that energy is not conserved during the shock (despite its inertial nature). This feature is also found in other interfacial flows dominated by inertia (such as the bursting of a soap bubble (Culick 1960)), and we showed qualitatively that a precise knowledge of the detail of the flow should help in understanding this problem, i.e. how energy is redistributed during the shock. This might define a stimulating program for future research in this field.

We thank S. T. Thoroddsen for his suggestions and for providing his original set of measurements. We also thank C. Aigle, A. L. Biance, F. Charru, F. Chevy, C. Colin, J. Magnaudet, K. Okumura and M. Provensal for discussions and help.

REFERENCES

Chandra, S. & Avedisian, C. T. 1991 *Proc. R. Soc. Lond.* A **432**, 13.

Culick, F. E. C. 1960 *J. Appl. Phys.* **31**, 1128.

Hartley, G. S. & Brunskill, R. T. 1958 In *Surface Phenomena in Chemistry and Biology* (ed. J. F. Danielli), p. 214. Pergamon.

Okumura, K., Chevy, F., Richard, D., Quéré, D. & Clanet, C. 2003 *Europhys. Lett.* **62**, 237.

Onda, T., Shibuichi, S., Satoh, N. & Tsujii, K. 1996 *Langmuir* **12**, 2125.

Rein, M. 1993 *Fluid Dyn. Res.* **61**, 769.

Richard, D. & Quéré, D. 2000 *Europhys. Lett.* **50**, 769.

Richard, D., Clanet, C. & Quéré, D. 2002 *Nature* **417**, 811.

Stow, C. D. & Hadfield, M. G. 1981 *Proc. R. Soc. Lond.* A **373**, 419.

Taylor, G. I. & Michael, D. H. 1973 *J. Fluid Mech.* **58**, 625.

Marmanis, H. & Thoroddsen, S. T. 1996 *Phys. Fluids* **8**, 1344.